Negative catalysis by the editing domain of class I aminoacyl-tRNA synthetases

Author names and affiliations

Igor Zivkovic[a], Kate Ivkovic[a], Nevena Cvetesic[b], Ita Gruic-Sovulj[a]

[a]Department of Chemistry, Faculty of Science, University of Zagreb, Horvatovac 102a, Zagreb 10 000, Croatia

[b]Institute for Clinical Sciences, Faculty of Medicine, Imperial College London and MRC London Institute of Medical Sciences, London SW7 2AZ, UK

Corresponding author information

I. Gruic-Sovulj, Department of Chemistry, Faculty of Science, University of Zagreb, Horvatovac 102a, Zagreb 10000, Croatia, Tel: +3851 4606230, E-mail: gruic@chem.pmf.hr

Keywords

Aminoacyl-tRNA synthetases, editing *in trans*, post-transfer editing, negative catalysis, amino acid specificity

Abstract

The faithful protein synthesis is a vital property of the cell as errors in translation can diminish cellular fitness and lead to severe neurodegeneration. Aminoacyl-tRNA synthetases (AARS) translate the genetic code by loading tRNAs with the cognate amino acids. The errors in amino acid recognition are cleared at the AARS editing domain through hydrolysis of misaminoacyl-tRNAs. Here, using *Escherichia coli* isoleucyl-tRNA synthetase (IleRS) as a model enzyme, we showed that the editing domain of class I AARSs does not select for non-cognate amino acids that jeopardize the AARS fidelity. Instead, it selects against the cognate aminoacyl-tRNA providing a new paradigm wherein safeguarding against misediting constrains the editing evolution. The specificity is established by the residues that promote negative catalysis through destabilisation of the transition state comprising exclusively the cognate amino acid. Such error-correction design is powerful as it allows broad substrate acceptance of the editing domain along with its exquisite specificity in the non-error rejection. This is set up by *in cis* substrate delivery to the editing domain, a fingerprint of class I but not class II AARSs. However, we found a gap in this class rule by unveiling that class I IleRS releases misaminoacyl-$tRNA^{Ile}$ and edits it *in trans*.

Introduction

Aminoacyl-tRNA synthetases (AARS) couple cognate amino acid and tRNA pairs for protein biosynthesis. They are divided into two, evolutionary distinct classes, class I and class II (Eriani et al., 1990; Ribas de Pouplana and Schimmel, 2001). In both classes, the pairing occurs at the synthetic active site by the same two-step mechanism bearing some class-dependent features (Zhang et al., 2006). The first step, amino acid activation, comprises the formation of aminoacyl-AMP (AA-AMP) while the second step is the transfer of the aminoacyl moiety to the tRNA (formation of aminoacyl-tRNA, AA-tRNA) **(Figure 1, paths 1 and 4)**. The coupling of non-cognate substrates leads to mistranslation, which can be toxic for the cell (Bilus et al., 2019; Cvetesic et al., 2014; Lee et al., 2006). Due to physicochemical similarities of cellular amino acids, around half of AARSs cannot achieve the tolerable level of fidelity (estimated to be 1 in 3300 (Loftfield and Vanderjagt, 1972)) in the synthetic reactions alone and thus have evolved editing (reviewed in (Gomez and Ibba, 2020; Perona and Gruic-Sovulj, 2014)). The error can be corrected by hydrolysis of non-cognate AA-AMP within the confines of the synthetic site (pre-transfer editing, **Figure 1, paths 2 and 3**) (Dulic et al., 2010; Gruic-Sovulj et al., 2007) and/or by hydrolysis of misaminoacyl-tRNA at the dedicated editing domain (post-transfer editing) (Lin et al., 1996; Silvian et al., 1999). The latter appears to be the dominant pathway, operating by two possible routes – *in cis* **(Figure 1, path 5 and 6)** and *in trans* **(Figure 1, path 7 - 9)** (Gomez and Ibba, 2020). Editing *in trans,* so far demonstrated only in class II AARS (Ling et al., 2009), entails dissociation of the AA-tRNA and its rebinding with the 3'-end facing the editing domain.

The interplay between the synthetic and editing sites was firstly addressed by Fersht's double-sieve hypothesis proposed originally for class I isoleucyl- (IleRS) and valyl-tRNA synthetases (ValRS) (Fersht and Dingwall, 1979a). It states that the synthetic site uses steric clash to discard larger than the cognate amino acids while the editing site clears smaller/isosteric non-cognate amino acids that were successfully aminoacylated to the tRNA. The steric clash was also proposed to prevent the binding of the cognate AA-tRNA to the editing domain. But, does the productive recognition at the editing site correlate well with the amino acid misrecognition at the synthetic site, and to what extent does the steric clash define the selectivity of the editing site? The former was anticipated but not experimentally addressed. The latter was tested to show that the selectivity against the cognate AA-tRNA arises from its imposed unproductive binding (Ahmad et al., 2015; Dulic et al., 2017; Hussain et al., 2010).

IleRS rapidly hydrolyses $tRNA^{Ile}$s misaminoacylated with non-proteinogenic norvaline (Nva) and Val (Bilus et al., 2019). This is expected as both Nva and Val are misactivated with a frequency that is 10-fold higher than the estimated tolerable error (Loftfield and Vanderjagt, 1972) and thus pose threats to the fidelity of Ile-$tRNA^{Ile}$ formation (Bilus et al., 2019; Fersht and Dingwall, 1979a). Surprisingly, IleRS can also efficiently hydrolyse $tRNA^{Ile}$ misaminoacylated with a non-proteinogenic α-aminobutyrate (Abu) and its synthetic γ-fluorinated analogues (F_2Abu and F_3Abu), which are misactivated with up to a 20-fold *lower* frequency than the estimated tolerable error (Zivkovic et al., 2020). This questions whether the editing site substrates need to be well misrecognized at the synthetic site, as anticipated.

Here, we set out to explore what shaped the selectivity of class I editing site and to unravel whether the same mechanisms and demands for selectivity are shared between the editing and the synthetic sites using IleRS as a model enzyme. We characterized amino acid activation and AA-$tRNA^{Ile}$ hydrolysis using a range of amino acids with different physicochemical properties (Ala, Ser, Thr, Met, Leu, Nle).

We found that IleRS synthetic site discriminates with at least 20 000-fold against the tested non-cognate amino acids. Thus, these substrates should not pose a fidelity problem. Nevertheless, all misaminoacylated $tRNA^{Ile}$s were rapidly hydrolysed (35-65 s^{-1}) at the editing site. Only cognate Ile-$tRNA^{Ile}$ was weakly hydrolysed, demonstrating that evolution of the editing site was driven by negative catalysis (Tawfik, 2014; Vögeli and Erb, 2018) *i.e.* selection towards destabilisation of the transition state for the cognate AA-tRNA hydrolysis (misediting). We also found that negative determinants for misediting vary among the closely related class I editing domains. Finally, we discovered that in IleRS, delivery of the AA-tRNA to the editing domain entails the accumulation of free AA-tRNA in solution, reminiscent of class II AARSs editing *in trans*.

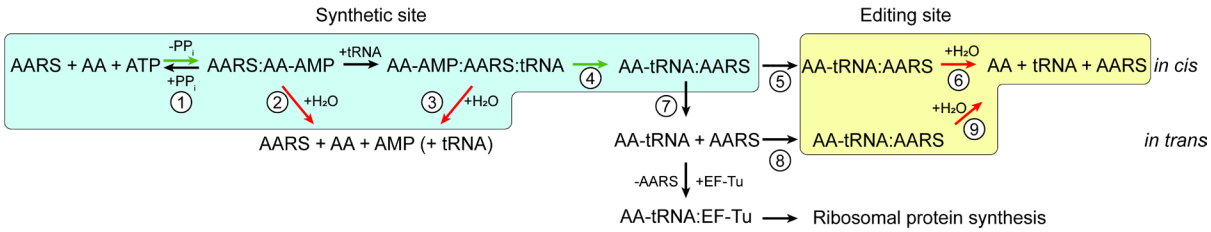

Figure 1. IleRS pathways of aminoacylation (green arrows) and editing (red arrows). The synthetic pathway consists of amino acid activation (1) and the aminoacyl transfer step (4). The editing pathways include tRNA-independent (2) and tRNA-dependent (3) pre-transfer editing and post-transfer editing (6, 9). Post-transfer editing can occur by translocation of AA-tRNA (5) to the editing domain for hydrolysis (6, *in cis*) or by AA-tRNA dissociation (7), its subsequent rebinding to the editing site (8) and hydrolysis (9, *in trans*).

Results

The editing site clears a broad range of misaminoacylated $tRNA^{Ile}$s

Misaminoacylation of $tRNA^{Ile}$ with the non-cognate amino acids that are significantly different from Ile (**Supplementary Figure S1**) is challenging. However, this is a prerequisite for addressing the selectivity of the editing site as post-transfer editing is tested by following hydrolysis of preformed misaminoacylated tRNAs (Cvetesic and Gruic-Sovulj, 2017). In doing so, we found that all tested non-cognate amino acids were activated (**Figure 1, path 1**) albeit with high discrimination factors (D > 20 000, **Table 1**), which reflect efficient exclusion of the non-cognate substrate from the IleRS synthetic site. This is in accordance with known high selectivity of the IleRS synthetic site (Bilus et al., 2019; Dulic et al., 2014; Fersht, 1977; Jakubowski and Fersht, 1981; Nakama et al., 2001; Tawfik and Gruic-Sovulj, 2020; Zivkovic et al., 2020). Somewhat surprisingly, despite weak misactivation, $tRNA^{Ile}$ was successfully misaminoacylated (up to 60 % aminoacylation level) with all tested non-cognate amino acids by post-transfer editing deficient T243R/D342A IleRS (Bilus et al., 2019; Dulic et al., 2010; Zivkovic et al., 2020) (**Supplementary Figure S2** and **Supplementary Figure S3**). Interestingly, we did not observe aminoacylation with WT IleRS (**Supplementary Figure S2, inset**). Thus, the editing deficient AARSs can provide an alternative to the ribozyme approach (Kourouklis et al., 2005) for tRNA misaminoacylation. This analysis is further complicated by artefacts that may arise from contamination of non-cognate amino acid samples with trace amounts of the cognate amino acids (Cvetesic et al., 2014; Fersht and Dingwall, 1979a, 1979b). For that reason, we estimated the purity of the used amino acids (**Supplementary Figure S4**) and found that Leu, and possibly also Met and Nle, may contain trace amounts of Ile.

Next, we isolated the post-transfer editing step by mixing preformed misaminoacylated $tRNA^{Ile}$ with a surplus of WT IleRS, using a rapid chemical quench instrument. The hydrolysis of misaminoacylated $tRNA^{Ile}$ was followed in time to calculate the first-order rate constant (**Supplementary Figure S3**). The single-turnover conditions ensure that product dissociation does not limit the observed rate (Cvetesic et al., 2012). A 2-fold higher concentration of IleRS or AA-$tRNA^{Ile}$ returned the same hydrolysis rate confirming that binding is not rate-limiting. Thus, the observed rate constants (**Figure 2**, **Supplementary Figure S3**) represent the catalytic step (hydrolysis of misaminocylated $tRNA^{Ile}$) within the editing site.

The single-turnover analysis revealed, in agreement with the incapacity of the WT IleRS to accumulate misaminoacylated $tRNAs^{Ile}$ (**Supplementary Figure S2, inset**), that all misaminoacylated-$tRNA^{Ile}$s were rapidly hydrolysed with similar rates ranging from 35 to 65 s^{-1} (**Figure 2**, please note that a possible Leu, Met and Nle contaminations did not compromise the editing analysis). This is surprising as these amino acids (except Val and Nva) are efficiently discriminated at the synthetic site and as such cannot pose a threat to IleRS aminoacylation fidelity. Finding that amino acids are rapidly cleared at the editing domain irrespectively of the requirement for their editing, lend a new paradigm about the editing selectivity principles. Moreover, the editing site shows no clear preference towards physicochemical features of the editing substrates, like size (Met and Nle, both with longer unbranched side chain, are eliminated), hydrophobicity (polar Ser and Thr are efficiently cleared at the editing site) or branching (Leu-$tRNA^{Ile}$ is also rapidly hydrolysed). Cognate Ile-$tRNA^{Ile}$ was the only exemption, suggesting, that prevention of cognate AA-tRNA misediting was a major constraint during

the evolution of the editing site. Thus, we set to explore how the editing site excludes the cognate Ile-tRNA^{Ile} and in parallel promotes editing of misaminoacylated tRNAs.

Table 1. Kinetic parameters for activation of amino acids by WT IleRS.

Amino acid	k_{cat} / s^{-1}	k_{sp}[a] / s^{-1} mM^{-1}	K_M / mM	D[b]
Ile	56.7 ± 0.3	(16.6 ± 0.4) × 10^3	(3.41 ± 0.06) × 10^{-3}	1
Val[c]	36 ± 6	77	0.47 ± 0.03	156
Nva[d]	41 ± 1	50	0.82 ± 0.07	239
Abu[e]	23 ± 3	1.6 ± 0.1	15 ± 1	10 375
Thr	32 ± 2	0.82 ± 0.04	39 ± 2	20 243
F_2Abu[e]	6.9 ± 0.7	0.45 ± 0.8	16 ± 2	36 888
F_3Abu[e]	5.3 ± 0.8	0.19 ± 0.02	28 ± 2	87 368
Ala	10 ± 1	0.10 ± 0.02	100 ± 9	166 000
Ser	-	0.016 ± 0.005[f]	-	1 037 500
Met	10.6 ± 0.4	7.6 ± 0.7	1.4 ± 0.1	NC[g]
Nle	4.8 ± 0.4	1.6 ± 0.2	3.1 ± 0.6	NC[g]
Leu	28.7 ± 0.7	26 ± 3	1.1 ± 0.1	NC[g]

The activation step was tested by ATP-PPi exchange assay. The values represent the average value ± SEM of at least three independent experiments.

[a]k_{sp} – specificity constant (k_{cat}/K_M) is obtained from the modified Michaelis-Menten equation $k_{obs} = \frac{k_{sp}[S]}{1+\frac{k_{sp}[S]}{k_{cat}}}$ (Johnson, 2019).

[b]Discrimination factor – $k_{sp,cognate}/k_{sp,non\text{-}cognate}$, *i.e.* $(k_{cat}/K_M)_{cognate}/(k_{cat}/K_M)_{non\text{-}cognate}$. The values below 3300 indicate higher error frequencies than the estimated error of protein synthesis (Loftfield and Vanderjagt, 1972).

[c]Data was taken from (Dulic et al., 2010). The k_{cat} and K_M values were determined using the unmodified form of the Michaelis-Menten equation. k_{sp} was calculated by dividing k_{cat} with K_M.

[d]Data was taken from (Bilus et al., 2019). The k_{cat} and K_M values were determined using the unmodified form of the Michaelis-Menten equation. k_{sp} was calculated by dividing k_{cat} with K_M.

[e]Raw data was taken from (Zivkovic et al., 2020).

[f]k_{cat} and K_M were not determined due to the low activity.

[g]Not calculated due to possible contamination of the amino acid sample with cognate Ile.

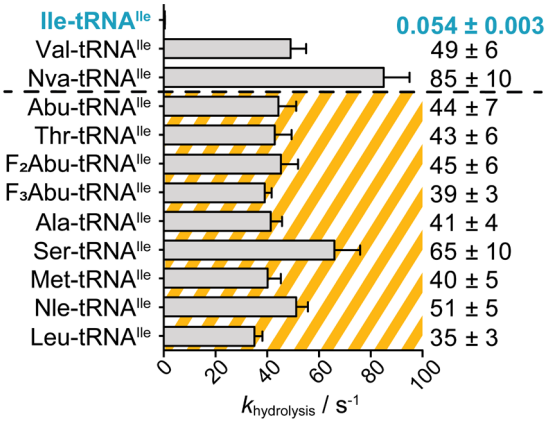

Figure 2. Single-turnover hydrolysis of misaminoacylated tRNAs by WT IleRS. tRNAs misaminoacylated with amino acids that are well discriminated at the IleRS synthetic site (D > 3300) are presented in the striped area. Value 3300 is taken as the tolerable error of protein synthesis was estimated around 1 in 3300 (Loftfield and Vanderjagt, 1972). Rapid hydrolysis of Leu-, Met-, and Nle-tRNA^{Ile} confirmed that possible traces of cognate Ile in the Leu, Met or Nle samples did not compromise the editing analysis. Time courses from which the first-order rate constants ($k_{hydrolysis}$) were calculated are presented in Supplementary Figure S3. $k_{hydroysis}$ for Val-, Nva-, Abu-, F$_2$Abu-, and F$_3$Abu-tRNAs^{Ile} were taken from (Bilus et al., 2019; Zivkovic et al., 2020).

Negative determinants for Ile-tRNA^{Ile} misediting

Two conserved residues of the editing domain, Thr246 and His333 (Thr233 and His319 in *T. thermophilus* IleRS, PDB ID: 1WNZ, **Supplementary Figure S5**) were previously characterised by time-course analysis and their equal contribution to the rejection of Ile-tRNA^{Ile} has been proposed (Fukunaga and Yokoyama, 2006; Hendrickson et al., 2002). However, in closely related LeuRS, the specificity against the cognate Leu resides solely on Thr252 (analogous to Thr246 in EcIleRS) (Dulic et al., 2017)**.** It has been shown that time-course analysis may lead to incorrect models of enzyme mechanisms (Dulic et al., 2010). Therefore, we used single-turnover catalysis to assign the individual contributions of Thr246 and His333 (**Table 2)**. Interestingly, T246A substitution, increased the rate of Ile-tRNA^{Ile} misediting by only 2-fold (0.126 ± 0.006 s^{-1}). In contrast, the H333A mutant showed a 20-fold increase in the rate of Ile-tRNA^{Ile} hydrolysis (1.04 ± 0.06 s^{-1}), arguing that, for IleRS, His333 is the main negative determinant of misediting. Finally, the T246A/H333A mutant showed a 260-fold increase in the rate of Ile-tRNA^{Ile} hydrolysis (14 ± 1 s^{-1}), displaying about 7-fold higher effect than the cumulative effects of the independent mutations. His333 was further mutated to Gly, which additionally increased the rate of Ile-tRNA^{Ile} hydrolysis (4-fold compared to H333A), suggesting that steric hindrance may contribute to the His333 action. Importantly, the mutants displayed only 2-fold slower rates of editing of non-cognate Val-tRNA^{Ile} relative to the WT (**Table 2**) pointing towards their almost exclusive effect on Ile-tRNA^{Ile} misediting. Thus, the main negative determinant of the IleRS editing site appears to be His333 whose role is synergistically supported by Thr246**.** This contrasts LeuRS which utilizes Thr252 as a sole negative determinant and suggests idiosyncratic evolution of the mechanisms governing rejection of the cognate product in class I editing domains.

Table 2. Single-turnover and steady-state rate constants for different variants of IleRS.

Enzyme	$k_{hydrolysis}$[a] / s^{-1}		$k_{aminoacylation}$[b] / s^{-1}
	Ile-tRNA^{Ile}	Val-tRNA^{Ile}	Ile
WT	0.054 ± 0.003	49 ± 6[c]	1.3 ± 0.2
T246A	0.126 ± 0.006	32 ± 2	1.5 ± 0.3
H333A	1.04 ± 0.06	19.2 ± 0.6	1.6 ± 0.4
H333G	4.4 ± 0.7	24 ± 1	1.1 ± 0.2
T246A/H333A	14 ± 1	24 ± 1	0.96 ± 0.06

The values represent the average value ± SEM of at least three independent experiments.
[a]Single-turnover rate constants for AA-tRNA^{Ile} hydrolysis. Time courses from which the first-order rate constants ($k_{hydrolysis}$) were calculated are presented in **Supplementary Figure S6**.
[b]Steady-state rate constants for Ile-tRNA^{Ile} synthesis.
[c]Data was taken from (Bilus et al., 2019).

IleRS deprived of the negative determinants misedits Ile-tRNA^{Ile} *in trans*

During steady-state (mis)aminoacylated AA-tRNA partitions between hydrolysis (editing; **Figure 1 path 6**) and dissociation (**Figure 1, path 7**) (product release). To reach the editing site, AA-tRNA translocates (**Figure 1, path 5**) its single-stranded 3' end while the tRNA body remains bound to the enzyme (editing *in cis*). In case when whole AA-tRNA dissociates from the enzyme prior reaching the editing site, it can re-bind from solution with the 3' end facing the editing domain (**Figure 1, paths 8 and 9,** editing *in trans*). Editing *in cis* depletes the product and thus compromises steady-state aminoacylation. In contrast, editing *in trans* may not affect the aminoacylation rate, because re-binding of AA-tRNA for hydrolysis is not favoured at low steady-state enzyme concentration. Therefore, the finding that both H333A and T246A/H333A IleRSs exhibit little to no change in steady-state aminoacylation rates relative to the WT enzyme ($k_{aminoacylation}$, **Table 2**), despite rapid Ile-tRNA^{Ile} hydrolysis at their editing sites ($k_{hydrolysis}$, **Table 2**), implies that these mutants misedit Ile-tRNA^{Ile} *in trans*. This is unexpected as editing *in trans* was not yet demonstrated for class I AARSs.

Non-stoichiometric ATP consumption is diagnostic of active editing as futile aminoacylation/editing cycles consume ATP without accumulating AA-tRNA. To address whether the IleRS mutants misedit Ile-tRNA^{Ile} *in trans*, two complementary approaches were undertaken: i) we used higher IleRS concentration (2 µM instead of 20 nM used in the steady-state aminoacylation) to favour re-binding of Ile-tRNA^{Ile} and thus misediting *in trans* and ii) higher IleRS concentration was complemented by the addition of 8-12 µM active EF-Tu, which may suppress misediting *in trans* by competing with IleRS in the binding of free Ile-tRNA^{Ile} (LaRiviere et al., 2001).

ATP consumption (AMP formation) and Ile-tRNA^{Ile} formation were followed in parallel reactions that differ only in the labelled components – [^{32}P]ATP was used for the former and [^{32}P]tRNA^{Ile} for the latter (**Supplementary Figure S7**). The ratio of consumed ATP per Ile-tRNA^{Ile} accumulated in solution (AMP/Ile-tRNA^{Ile}) was calculated for the reactions without and with EF-Tu (**Figure 3**). In the absence of EF-Tu, both mutants consume 18- (H333A) to 1100-fold (T246A/H333A) higher than the stoichiometric amount of ATP per released Ile-tRNA^{Ile}. Thus, multi-turnover conditions at high concentrations of the mutants support misediting. That misediting takes place *in trans*, is further supported by 9- (H333A) to 18-fold (T246A/H333A) drop in AMP/Ile-tRNA^{Ile} ratio in the presence of EF-Tu. The WT enzyme, exhibiting marginal Ile-tRNA^{Ile} misediting, used stoichiometric amount of ATP per Ile-tRNA^{Ile}, independently on the presence/absence of EF-Tu. Interestingly, the significant

energetic cost of misediting was exhibited mainly with T246A/H333A, raising an intriguing question - how detrimental is hydrolysis of Ile-tRNA^{Ile}?

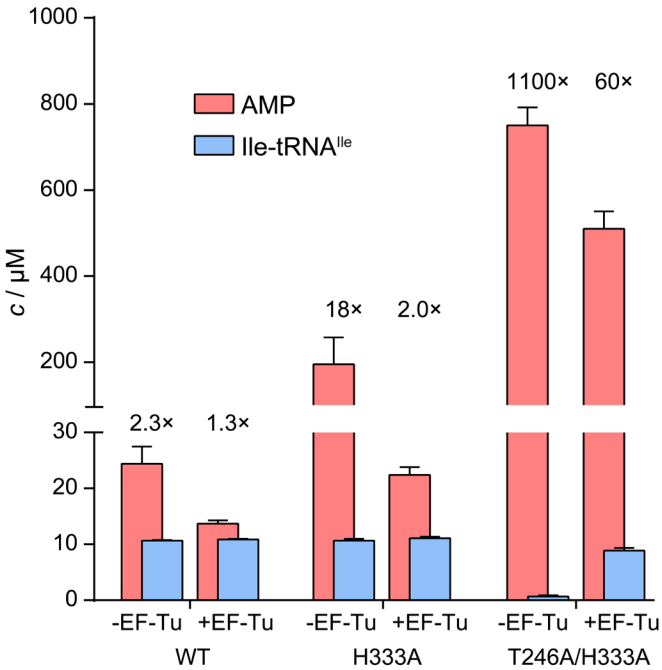

Figure 3. AMP (pink) and Ile-tRNA^{Ile} (blue) concentrations at the 5-minute time point for WT, H333A and T246A/H333A IleRS. The time courses are given in Supplementary Figure S7. The numbers above bars are AMP/Ile-tRNA^{Ile} ratios. The enzymes were 2 µM, the tRNA^{Ile} 12 µM, and EF-Tu (the active GTP-form) was 8-12 µM.

Ile-tRNA^{Ile} misediting impairs cell growth

To investigate to what extent misediting of Ile-tRNA^{Ile} affects cell viability, we followed the growth of *E. coli* BL21(DE3) strain transformed with the plasmids encoding WT IleRS or its Ile-tRNA^{Ile} misediting active variants (H333A and T246A/H333A). A moderate expression (**Supplementary Figure S8**) of the WT enzyme did not show any growth defects demonstrating that expression *per se* is not a burden for the cell (**Figure 4**). Interestingly, the H333A mutant did not significantly influence the growth rate suggesting that Ile-tRNA^{Ile} misediting of 1 s^{-1} could be physiologically tolerated. In contrast, the T246A/H333A mutant (hydrolytic rate of 14 s^{-1}) showed a noticeable growth defect (**Figure 4**), in agreement with the negative selection against this activity.

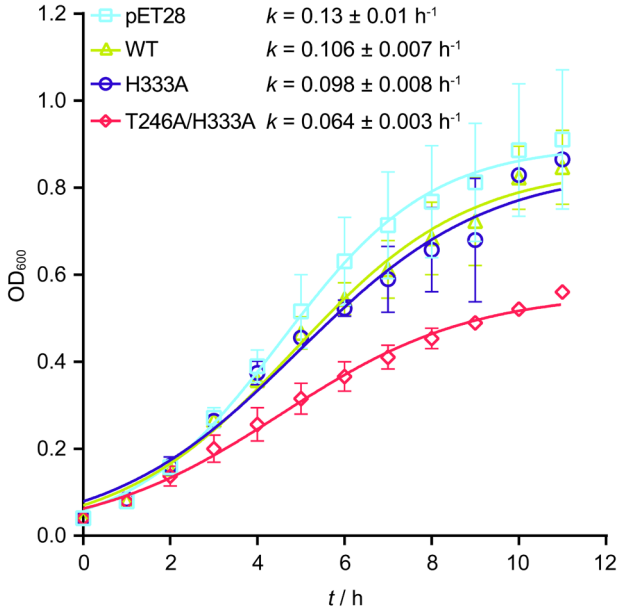

Figure 4. Growth of *E. coli* BL21(DE3) transformed with the pET28 plasmids carrying IleRS variants. The empty plasmid was used as a control. The growth was followed in M9 medium supplemented with 100 µM IPTG. The growth rate constant (*k*) was determined from the logistic growth model. In the absence of IPTG, the growth rate of *E. coli* BL21(DE3) transformed with the empty pET28 was 0.28 ± 0.01 h^{-1}. The basal level of Ile-$tRNA^{Ile}$ synthesis by endogenous WT IleRS should not pose a problem as Ile-$tRNA^{Ile}$ produced by any route is subjected to editing *in trans*.

IleRS is unique among class Ia AARSs in exhibiting a high level of editing *in trans*

To address whether IleRS edits *in trans* its biological threat Val-$tRNA^{Ile}$, we followed the accumulation of AMP and Val-$tRNA^{Ile}$ by the WT enzyme as described above bearing in mind that EF-Tu may bind tRNAs misaminoacylated with near-cognate amino acids (Cvetesic et al., 2013; Ling et al., 2009, 2007b). In the absence of EF-Tu, the analysis returned the AMP/Val-$tRNA^{Ile}$ ratio of 1330 and a minor accumulation of Val-$tRNA^{Ile}$ (**Figure 5, Supplementary Figure S9**), both in agreement with the efficient Val-$tRNA^{Ile}$ editing (Cvetesic et al., 2015). The addition of EF-Tu increased the accumulation of Val-$tRNA^{Ile}$ by 10-fold and decreased the amount of consumed ATP by more than 3-fold, leading to a significant drop (58-fold) in AMP/Val-$tRNA^{Ile}$ ratio (23 *vs* 1330). This indicates that IleRS edits Val-$tRNA^{Ile}$ *in trans*, providing to the best of our knowledge the first demonstration of editing *in trans* for a class I AARS.

Next, we tested whether LeuRS and ValRS also use editing *in trans* with their main biological threats Nva and Thr, respectively (Cvetesic et al., 2014; Fersht and Kaethner, 1976). Both LeuRS and ValRS consumed a highly non-stoichiometric amount of ATP per accumulated misaminoacylated tRNA (14 500 and 13 800, **Figure 5, Supplementary Figure S9**), in agreement with established editing of Nva-$tRNA^{Leu}$ and Thr-$tRNA^{Val}$ (Bilus et al., 2019; Cvetesic et al., 2012; Fersht and Kaethner, 1976). The addition of EF-Tu dropped the ATP/ Thr-$tRNA^{Val}$ ratio by less than 2-fold (13 800 *vs* 8600). The lack of EF-Tu effect indicates that ValRS edits Thr-$tRNA^{Val}$ *in cis*. The picture is more complicated for LeuRS, where the presence of EF-Tu promotes a 12-fold drop in ATP/AA-tRNA ratio (14 500 *vs* 1250) that may indicate the participation of editing *in trans*. However, the drop does not stem from a decrease in the ATP consumption, which is only 1.04-fold lower in the presence of EF-Tu. Thus, the cycles of Nva-$tRNA^{Leu}$ hydrolysis and the subsequent $tRNA^{Leu}$ misaminoacylation which consumes ATP are not

influenced by EF-Tu. This strongly suggests that LeuRS mainly operates *in cis* in agreement with the previous data (Ling et al., 2009). The observed EF-Tu-dependent accumulation of AA-tRNA^{Leu} is puzzling and likely originates from trace contaminations of Leu in the Nva sample (**Supplementary Figure S10**). Indeed, the accumulation of Leu-tRNA^{Leu}, like of Nva-tRNA^{Leu} can be diminished by rebinding to LeuRS and (mis)editing. Yet, hydrolysis of Leu-tRNA^{Leu} is 3×10^3-times slower than Nva-tRNA^{Leu} (Cvetesic et al., 2012), contributing minimally to the ATP consumption. EF-Tu may bind Leu-tRNA^{Leu} and thus affects its accumulation but without a noticeable effect on ATP consumption. To conclude, our data show that IleRS is distinct from closely related LeuRS and ValRS in a fraction of post-transfer editing that operates *in trans*.

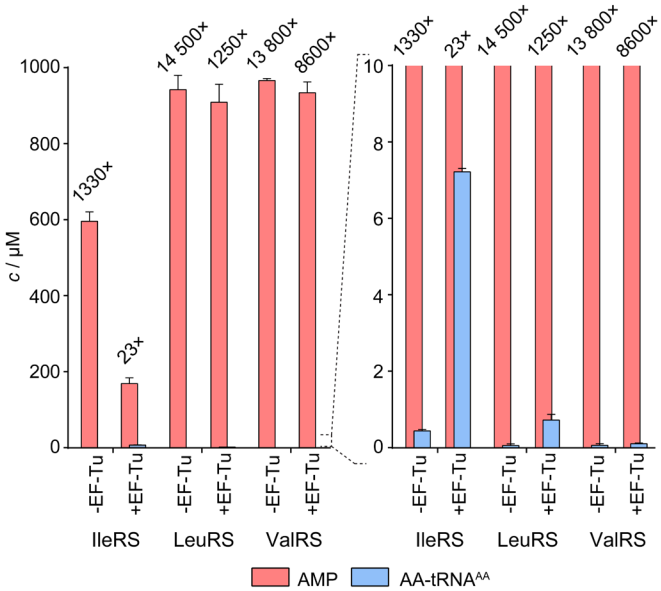

Figure 5. AMP (pink) and misaminoacylated tRNA (blue) concentrations at the 5-minute time point for IleRS, LeuRS and ValRS. The time courses are given in Supplementary Figure S9. The numbers above bars are AMP/Ile-tRNA^{Ile} ratios. The enzymes were 2 µM, the tRNAs 10 µM, and EF-Tu (the active GTP-form) was 8-12 µM.

Discussion

Class I AARS synthetic and editing sites act as mirror images

AARSs are textbook examples of how high selectivity emerged under strong evolutionary pressure to evade deleterious errors (Tawfik and Gruic-Sovulj, 2020). Their synthetic sites adopt numerous strategies to enforce recognition of the cognate and rejection of the non-cognate amino acids (Arnez et al., 1999; Fersht et al., 1985; Newberry et al., 2002; Sankaranarayanan et al., 2000). If non-cognate amino acid, however, gets coupled to the tRNA, post-transfer editing resolves the problem. The editing site evolved to clear amino acids that jeopardize the accuracy of translation arguing that amino acids well discriminated at the synthetic site (large discrimination factor, *D*) will be poorly edited. But is it so? What did actually shape selectivity of the editing domain? We used IleRS as a model enzyme and a series of amino acids of distinct physicochemical features and evolutionary origin to address these questions.

We surprisingly found that tRNAs misaminoacylated with non-cognate amino acids that are efficiently discriminated at the activation step (**Table 1**) were all edited with the same rates as the biological threats Nva- and Val-tRNA^{Ile} (**Figure 2**). This demonstrates that recognition at the editing site is not influenced by how well the non-cognate amino acid is discriminated at the synthetic site. The similar was found for ValRS (Bilus et al., 2019) and LeuRS (Cvetesic et al., 2014, 2012). It appears that the editing site is non-selective (except for the cognate AA-tRNA) and hydrolyses tRNAs misaminoacylated with amino acids spanning a broad range of physicochemical properties. How is this possible? The substrate recognition and catalysis at the class I editing site relies on the common parts of all AA-tRNAs; the terminal adenosine of the tRNA (A76) and α-NH_3^+ group of the amino acid attached to the tRNA anchor the substrates (Fukunaga and Yokoyama, 2006) while the 2'OH or 3'OH group of the A76 acts as a general base and promotes catalysis (shown for class I (Cvetesic et al., 2015; Dulic et al., 2017) and class II (Ling et al., 2007a; Minajigi and Francklyn, 2008)). Changes of the terminal adenosine (Tardif et al., 2001), lack of 2'OH or 3'OH (Cvetesic et al., 2015; Dulic et al., 2017; Ling et al., 2007a; Minajigi and Francklyn, 2008) or loss of the α-NH_3^+ anchoring interactions deprived editing (Bishop et al., 2002; Cvetesic et al., 2012). Thus, it is plausible to assume that a common tRNA carrier and preselection of the editing substrates by the aminoacylation sieve, could have driven the evolution of the editing domain towards a broad substrate acceptance and the lack of recognition of the non-cognate amino acid's side chain. In contrast, the synthetic site, acting as the first sieve, recognizes standalone amino acid and uses most of its side chain (**Table 1**) to minimize the error and ATP consumption (editing) (Tawfik and Gruic-Sovulj, 2020). Thus, the synthetic and editing sites act as mirror images; while the former is highly selective to prevent errors, the latter exhibits low selectivity to clear each non-cognate amino acid that comes loaded to the tRNA.

Finding that class II PheRS, which recognizes the functional group of Tyr at the editing site (Kotik-Kogan et al., 2005) edits Ile-tRNA^{Phe} (Yarus, 1972), indicates that broad selectivity is not confined only to the class I editing domain. Further, D-aminoacyl-tRNA deacylase, which bears a structural resemblance to the archaeal class II threonyl-tRNA synthetase editing domain (Dwivedi et al., 2005), edits all D-amino acids at similar rates while efficiently rejecting L-amino acids. (Routh et al., 2016). In contrast, the editing domain (INS) of class II prolyl-tRNA synthetase (ProRS), as well as the free-standing bacterial ProRS INS domain homologs, have well-defined non-cognate amino acid specificity (Bacusmo et al., 2017). Interestingly, the free-standing *trans*-editing proteins also evolved a broad specificity – in this case regarding the tRNA substrate (Liu et al., 2015). Thus, across the editing systems, a similar concept

emerged independently arguing for the benefits of broad substrates acceptance in the design of the efficient error correction mechanisms.

Negative catalysis ensures high specificity and broad selectivity of class I editing domain

Enzymes significantly differ in their physiological requirements for high selectivity (Tawfik and Gruic-Sovulj, 2020). In some cases, low selectivity is beneficial allowing a broad substrate scope as in cytochrome P450 (Durairaj et al., 2016). The same applies to the editing domain. Yet, a unique feature of the editing domain, in which it mirrors highly selective enzymes (Johnson, 2008), is its exquisite specificity *in rejection* of the cognate AA-tRNA. In general, specificity may evolve by positive and negative selection (Tawfik, 2014). While the former is a consequence of a selection for the enzyme's high catalytic efficiency towards the cognate substrate, the latter is an explicitly evolved trait against a particular non-cognate substrate to avoid deleterious errors. Here we propose that specificity of the editing domain evolved through negative selection against the cognate AA-tRNA. We and others have previously shown that the cognate AA-tRNA is rejected from the editing site not by mitigating the binding, but by diminishing the catalysis (Ahmad et al., 2015; Dulic et al., 2017; Hussain et al., 2010; Ling et al., 2009). Destabilisation of the transition state solely for cognate AA-tRNA hydrolysis can be viewed as an example of negative catalysis (Vögeli and Erb, 2018). This concept was introduced to explain that alongside promoting a wanted reaction by lowering the energy of the transition state for the desired product (positive catalysis), enzymes may also increase the energy barrier of the competing transition state preventing the side reaction (negative catalysis). Herein, we broaden this concept to compare transition states for the competing substrates. Thus, the residue conferring negative catalysis should not influence the rate of native (wanted) reaction but should diminish the reaction rate with the prohibited substrate. Visualisation of our data by activity-specificity graph revealed that the His333 and Thr246 IleRS residues confer negative catalysis (**Figure 6**). Their substitutions do not influence editing of Val-tRNA^{Ile} (k_{mut}/k_{WT} for editing is close to one) but promote misediting of Ile-tRNA^{Ile} resulting in the variants with decreased specificity (drop in the ratio of the k_{mut}/k_{WT} values for editing over misediting). In contrast, D342A mutation in IleRS promoted a decrease in both activity and specificity conferring the positive role for the Asp342 residue in catalysis (promoting both wanted and unwanted reaction by anchoring α- NH_3 of the cognate and non-cognate amino acid (Cvetesic et al., 2015; Fukunaga and Yokoyama, 2006)). Similarly, LeuRS Thr252, which imposes unproductive positioning of Leu-tRNA^{Leu} (Dulic et al., 2017), confers negative catalysis while the Asp345 residue (Cvetesic et al., 2012), analogous to IleRS Asp342, promotes positive catalysis. In conclusion, negative selection/catalysis appears as a powerful mechanism to ensure low selectivity of the editing domain while keeping, at the same time, exquisite specificity in the rejection of the cognate AA-tRNA. The former was driven by relying on the common parts of all AA-tRNAs and the latter by the

evolution of a specific kinetic rejection mechanism based on the cognate amino acid side chain (Ahmad et al., 2015; Dulic et al., 2017; Hussain et al., 2010).

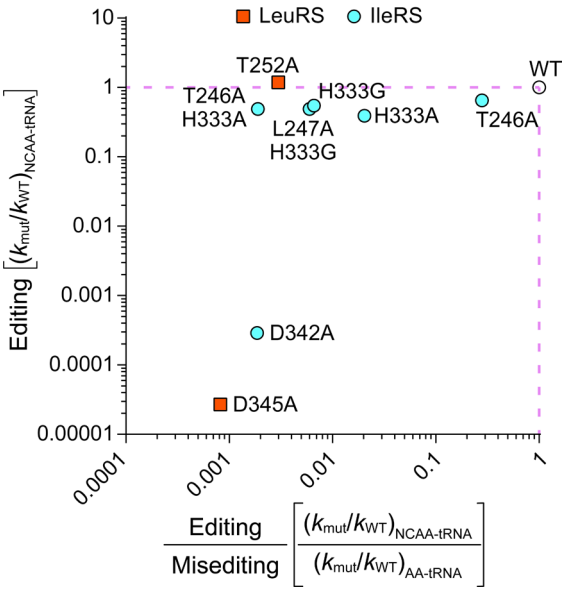

Figure 6. Activity-specificity relationship for editing of IleRS and LeuRS mutants. Activity (editing) was calculated as the ratio of the rate constants for hydrolysis of misaminoacylated tRNAs (NCAA-tRNA) by mutant AARS and WT, respectively. Specificity was calculated as the ratio of editing (wanted) over misediting (unwanted), where the misediting is the ratio of the rate constants for hydrolysis of cognate AA-tRNAs by mutant AARS and WT, respectively.

IleRS – class Ia enzyme with unique editing features

In class I AARSs, delivery of the amino acid from the synthetic to the editing site occurs through fast translocation (estimated as faster than 80 s^{-1} in LeuRS (Cvetesic et al., 2012)) of the 3'-end of the (mis)aminoacylated tRNA (Palencia et al., 2012) (**Figure 1**). The fast translocation allows that the 3'-end reaches the editing site on a shorter time scale relative to the rate-limiting dissociation of the (mis)aminoacylated tRNA. Therefore, editing occurs *in cis* without the release of misaminoacylated tRNA. Release and rebinding of the misaminoacylated tRNAs to AARS was shown so far only for class II AARS (Ling et al., 2009), and was attributed to fast dissociation of (mis)aminoacylated tRNA (Zhang et al., 2006). It, therefore, came as a surprise that IleRS edits Val-$tRNA^{Ile}$ with a significant contribution of the *in trans* pathway. At the same time, both LeuRS and ValRS predominantly operate *in cis* (**Figure 5**). Thus, IleRS appears unique among closely related class Ia editing AARSs (ILVRS) in post-transfer editing. Although the mechanistic basis is still missing, it is worth commenting here that only IleRS, among ILVRS, uses tRNA to both optimize the affinity for the amino acid substrate and to stimulate pre-transfer editing (**Figure 1, path 3**). Indeed, *E. coli* IleRS showed substantial tRNA-dependent pre-transfer editing that comprises about 30 % of total editing (Cvetesic et al., 2012; Dulic et al., 2014, 2010). Thus, an idiosyncratic utilisation of the tRNA as a co-factor may influence the rates of the tRNA-dependent steps, for example translocation.

It has been shown that PheRS can compete with EF-Tu for binding to Tyr-$tRNA^{Phe}$ (Ling et al., 2009) providing a basis for editing *in trans*. In our hands, EF-Tu efficiently competes with IleRS for binding to Val-$tRNA^{Ile}$, but the experimental set up was designed to promote the EF-Tu interaction. Further, this *in vitro* observation is distinct from *in vivo* environment where other AA-tRNAs compete for EF-Tu. Nevertheless, it is plausible to assume that editing *in trans* is generally of lower proficiency than editing *in cis*, because EF-Tu may bind tRNAs misaminoacylated with amino acids similar to the cognate one (Cvetesic et al., 2013; Ling et al., 2009, 2007b) and redirect them to ribosomal translation. That said,

IleRS capacity to edit errors prior misaminoacylation could be relevant opening a provocative question to what extent is AA-tRNA leakage and its editing *in trans* intertwined with pre-transfer editing.

Materials and Methods

Purification of IleRS, LeuRS, and ValRS

IleRS (EC 6.1.1.5) variants were produced using QuikChange (Agilent) mutagenesis and mutations were confirmed by sequencing. Genes for *E. coli* IleRS (wild-type and mutants), LeuRS (EC 6.1.1.4) and ValRS (EC 6.1.1.9) inserted into pET28b plasmid were overexpressed in *E. coli* BL21(DE3) and purified by affinity chromatography on Ni-NTA resin (Cytiva) as described (Cvetesic et al., 2012; Dulic et al., 2010). IleRS and ValRS were additionally purified to remove AA-AMP which is copurified bound in the enzyme active site as described (Zivkovic et al., 2020).

Purification and activation of the EF-Tu

The elongation factor Tu (EF-Tu, EC 3.6.5.3) with the C-terminal His-tag was overexpressed in *E. coli* BL21(DE3). Cells were grown to OD_{600} of 0.6-0.8 at 37 °C and expression was induced with 0.2 mM IPTG for 3 h. EF-Tu was purified on Ni-NTA resin (Cytiva) as described previously (Cvetesic et al., 2013). EF-Tu was stored as the inactive GDP-bound form at -20 °C in a buffer containing 50 mM Hepes pH =7.5, 10 mM $MgCl_2$, 50 mM KCl, 50 % glycerol, 50 µM GDP and 5 mM β-mercaptoethanol. Activation of the EF-Tu:GDP was performed in 70 mM Hepes pH = 7.5, 50 mM ammonium acetate, 10 mM magnesium acetate, 30 mM KCl, 0.8 mM DTT, 10 mM phosphoenolpyruvate, 1 mM GTP and 0.08 U/µL pyruvate kinase (Sigma) at 37 °C for 2 hours. EF-Tu:GTP was used immediately after the activation. The activation is not efficient and results in about 10-15 % of the total EF-Tu being capable of AA-tRNA binding (Cvetesic et al., 2013; Nazarenko et al., 1994; Sanderson and Uhlenbeck, 2007). Thus, the herein reported concentrations of EF-Tu presents the form capable of binding AA-tRNA (10-15 % total concentration of EF-Tu).

Purification and labelling of tRNAs

Synthetic genes for $tRNA^{Ile}_{GAT}$ (with G1–C72 instead of WT A1–U72 sequence), $tRNA^{Leu}_{TAA}$ and $tRNA^{Val}_{TAC}$ inserted into the pET3a plasmid were overexpressed in *E. coli* BL21(DE3) (Cvetesic et al., 2012; Dulic et al., 2010). Cells were grown to OD_{600} of 0.5-0.6 at 37 °C and expression was induced with 1 mM IPTG overnight at 30 °C. Substitution of the first base pair enhances transcription and does not affect $tRNA^{Ile}$ participation in the IleRS synthetic and editing reactions (Cvetesic et al., 2015; Nureki et al., 1994). tRNAs were isolated and purified by phenol/chloroform extraction, PEG_{8000} precipitation (removal of high molecular weight nucleic acids) and ethanol precipitation as described previously (Dulic et al., 2010). Purified $tRNA^{Leu}$ and $tRNA^{Val}$ had acceptor activity > 90 %. The acceptor activity of $tRNA^{Ile}$ was around 50 % so it was subjected to further purification by reverse phase chromatography on a semi-preparative Jupiter C4 column (Phenomenex), as described (Dulic et al., 2010), which increased the acceptor activity to 80-90 %. tRNAs were stored in 5 mM Hepes pH 7.5. Before further use $tRNA^{Leu}$ and $tRNA^{Val}$ were renaturated by heating at 85 °C for 3 min, adding an equal volume of pre-heated 20 mM $MgCl_2$, and slow cooling to room temperature for about 1 h. Labelled [^{32}P]tRNAs were prepared as described (Cvetesic and Gruic-Sovulj, 2017; Wolfson and Uhlenbeck, 2002). [^{32}P]tRNAs had acceptor activity 75-90%.

Preparation of misaminoacylated tRNAs

Misaminoacylated [^{32}P]tRNAs were prepared by mixing 25 µM tRNA^{Ile} with 5 µM T243R/D342A IleRS (mutant inactive in post-transfer editing) and a particular amino acid at the following concentration (4 mM Ala or Met; 2 mM Val, Nle or Thr; 0.2 mM Leu; 10 mM Ser) in a buffer containing 20 mM Hepes pH 7.5, 10 mM $MgCl_2$, 150 mM NH_4Cl, 2 mM ATP, 0.008 U/µL thermostable inorganic pyrophosphatase (TIPP, Sigma), 0.01 mg/mL BSA (New England Biolabs). All amino acids were purchased from Sigma. Amino acids were added in a moderate amount to prevent aminoacylation with possible Ile contaminations in the non-cognate amino acid samples. Reactions were quenched after 30 min at 37 °C by mixing with an equal amount of phenol/chloroform. AA-tRNA^{Ile}s were purified by phenol/chloroform extraction followed by two consecutive steps on Bio-Spin P30 columns (Bio-Rad) and dialyzed against 10 mM NaOAc pH 4.5. Before further use AA-tRNA^{Ile}s were renaturated by heating at 85 °C for 3 min, adding an equal volume of pre-heated 20 mM $MgCl_2$, and slow cooling (around 1 h) to room temperature.

Amino acid activation

Amino acid activation was followed by an ATP-PP_i exchange assay (Calendar and Berg, 1966; Cole and Schimmel, 1970; Francklyn et al., 2008) which was performed at 37 °C in a buffer containing 50 mM Hepes pH 7.5, 20 mM $MgCl_2$, 0.1 mg/mL BSA, 5 mM DTT, 4 mM ATP and 1 mM [^{32}P]PP_i (Perkin-Elmer). Enzymes were present at 50 to 100 nM while amino acid concentrations were varied from 0.1 to 10 × K_M. Reactions were quenched by mixing 1.5 µL of the reaction mixture with 3 µL of the quench solution (600 mM NaOAc pH 4.5 and 0.15 % SDS). Formed [^{32}P]ATP was separated from the remaining [^{32}P]PPi by thin-layer chromatography (TLC) on polyethyleneimine plates (Macherey-Nagel) in 4 M urea and 750 mM KH_2PO_4 pH 3.5. Signal visualization was performed on a Typhoon Phosphoimager (GE Healthcare) and quantified with ImageQuant software as described (Cvetesic and Gruic-Sovulj, 2017). Kinetic parameters (k_{cat} and k_{sp}) were obtained by fitting the data to the modified Michalis-Menten equation: $k_{obs} = \frac{k_{sp}[S]}{1+\frac{k_{sp}[S]}{k_{cat}}}$, where k_{cat} is the turnover number, k_{sp} is the specificity constant (k_{cat}/K_M), [S] is the amino acid concentration and k_{obs} is the observed rate constant. k_{obs} is calculated as $v_0/[E]_0$, where v_0 is the initial reaction rate and $[E]_0$ is the enzyme concentration. The data were fitted using GraphPad Prism software. We opted for the modified Michaelis-Menten equation due to the benefits discussed recently by K. Johnson (Johnson, 2019). Briefly, by fitting the data to the modified model, k_{sp} is obtained directly, rather than being calculated from k_{cat} and K_M, which leads to smaller errors.

Two-step aminoacylation

Aminoacylation of tRNA^{Ile}, comprising both activation and the transfer step, by various IleRS variants was followed at 37 °C in a buffer containing 20 mM Hepes pH 7.5, 10 mM $MgCl_2$, 150 mM NH_4Cl, 2 mM ATP, 0.008 U/µL TIPP and 0.01 mg/mL BSA, 15 µM tRNA^{Ile} 1 mM Ile and 20 nM WT, T246A, H333A, H333G, T246A/H333A or L247A/H333G IleRS. Misaminoacylation of tRNA^{Ile} was followed under the same conditions except that the concentrations of enzymes were higher (1 µM WT or T243R/D342A IleRS) and non-cognate amino acids were used at following concentrations: Leu 0.2 mM; Nle and Thr 2 mM; Ala and Met 4 mM; Ser 10 mM. The reactions were stopped by mixing 1.5 µL of the reaction mixture with 3 µL of the quench solution (600 mM NaOAc pH 4.5 and 0.15 % SDS). 1.5 µL of the quenched reaction mixture was mixed with 3 µL of P1 nuclease (Sigma) (≥0.01 U/µL in 300 mM NaOAc

pH 5.0 and 0.15 mM $ZnCl_2$) and incubated for 1 hour at room temperature. The P1 nuclease treatment releases terminal adenine nucleotide, with or without amino acid attached as the result of tRNA aminoacylation. Free and aminoacylated [^{32}P]AMP were separated by TLC in 100 mM NaOAc and 5 % HOAc. Signal visualization was performed on a Typhoon Phosphoimager (GE Healthcare) and quantified with ImageQuant software as described (Cvetesic and Gruic-Sovulj, 2017).

Parallel Formation of AMP and AA-tRNA

Formation of [^{32}P]AMP and AA-[^{32}P]tRNA were followed at 37 °C in parallel reactions, in a buffer containing 50 mM Hepes 7.5, 20 mM $MgCl_2$, 0.1 mg/mL BSA and 2 mM DTT supplemented with 0.1 mg/mL BSA, 1 mM ATP and 0.004 U/µL thermostable inorganic pyrophosphatase and 10-12 µM tRNA. The reactions that monitored [^{32}P]AMP formation were supplemented with [α-^{32}P]ATP (0.01-0.1 mCi/mL) (Perkin Elmer) while the reactions that monitored AA-[^{32}P]tRNA were supplemented with [^{32}P]tRNA (0.01-0.1 mCi/mL). The enzymes were 2 µM and amino acids were used at the following concentrations: 2 mM Ile, 20 mM Val and 30 mM Nva or Thr. The concentration of the GTP-bound EF-Tu, when added, was estimated to 8-12 µM (total concentration of added EF-Tu was 80 µM). The reactions were stopped by mixing 1.5 µL of the reaction mixture with 3 µL of the quench solution (600 mM NaOAc pH 4.5 and 0.15 % SDS). For following AMP formation, [^{32}P]ATP and [^{32}P]AMP were separated by TLC in 100 mM NaOAc and 5 % HOAc. When the formation of AA-tRNAs was followed, the quenched reaction mixtures were degraded by P1 nuclease and separated as described for the two-step aminoacylation (see above). Signal visualization was performed on a Typhoon Phosphoimager (GE Healthcare) and quantified with ImageQuant software as described (Cvetesic and Gruic-Sovulj, 2017).

Single-turnover hydrolysis

Single-turnover hydrolysis of AA-tRNAs was performed at 37 °C by mixing equal volumes of 20 µM IleRS in a buffer containing 200 mM Hepes pH 7.5, 75 mM NH_4Cl, 20 mM $MgCl_2$, 5 mM DTT and 0.01 mg/mL BSA and freshly renaturated misaminoacylated [^{32}P]tRNA^{Ile} (0.2-1 µM) in 10 mM NaOAc pH 4.5 as described previously (Zivkovic et al., 2020). Mixing of the enzyme and AA-[^{32}P]tRNAs was done using a rapid chemical quench instrument (RQF-3, KinTek Corp.). For the reactions having $t_{1/2} \geq 5$ s, manual mixing was performed. The reaction mixtures were quenched, treated with P1 nuclease, AA-[^{32}P]AMP and [^{32}P]AMP were separated and analysed as described for the aminoacylation (see above and (Cvetesic and Gruic-Sovulj, 2017)). The data were fitted to the single exponential equation $Y = Y_0 + A \times e^{-k_{hydrolysis} \times t}$, where Y_0 is the y intercept, A is a scaling constant, $k_{hydrolysis}$ is the apparent hydrolytic rate constant, and t is time.

Effect of the expression of IleRS variants on the growth of *E. coli*

E. coli BL21(DE3) strain was transformed with pET28 plasmids carrying genes for either WT IleRS, H333A IleRS or T246A/H333A IleRS. The empty plasmid was used as a control. The cultures were grown in 100 mL culture flasks in the M9 media with the addition of 0.4 % glucose and 30 µg/mL kanamycin. Overnight cultures were diluted to OD_{600} of 0.04 and supplemented with 100 µM IPTG to induce the protein expression. The growth at 37 °C and 250 rpm was monitored using UV-Vis spectrophotometer Evolution 60S (Thermo Scientific). The expression profile was followed by SDS-PAGE. The data were

fitted to the logistic model $y = \frac{A}{1+e^{\left(4\times\frac{k}{A}(\lambda-t)+2\right)}}$, where A is the maximal cell growth, λ is the lag phase and k is the growth rate constant.

Acknowledgments

We gratefully acknowledge Marko Mocibob, Vladimir Zanki and Vijay Jayaraman for fruitful discussions and comments regarding this manuscript. Ita Gruic-Sovulj dedicates this manuscript to the memory of Dan Salah Tawfik, whose generosity, creativity, and passion for life and science will continue to inspire many of us.

Competing interests

No competing interests declared.

Funding

This work was supported by Croatian Science Foundation Grant IP-2016-06-6272 and the Swiss Enlargement Contribution in the framework of the Croatian-Swiss Research Programme, Grant IZHRZ0_180567.

Author contributions

I.Z. and I.G.-S. designed research; I.Z. and K.I. performed research; I.Z., K.I. and I.G.-S. analysed data, N.C. performed preliminary research; I.Z., N.C. and I.G.-S. wrote the manuscript, I.G.-S. conceived and conducted the project.

References

Ahmad S, Muthukumar S, Kuncha SK, Routh SB, Yerabham ASK, Hussain T, Kamarthapu V, Kruparani SP, Sankaranarayanan R. 2015. Specificity and catalysis hardwired at the RNA-protein interface in a translational proofreading enzyme. *Nat Commun* **6**:1–12. doi:10.1038/ncomms8552

Arnez JG, Dock-Bregeon AC, Moras D. 1999. Glycyl-tRNA synthetase uses a negatively charged pit for specific recognition and activation of glycine. *J Mol Biol* **286**:1449–1459. doi:10.1006/jmbi.1999.2562

Bacusmo JM, Kuzmishin AB, Cantara WA, Goto Y, Suga H, Musier-Forsyth K. 2017. Quality control by *trans* -editing factor prevents global mistranslation of non-protein amino acid α-aminobutyrate. *RNA Biol* 1–10. doi:10.1080/15476286.2017.1353846

Bilus M, Semanjski M, Mocibob M, Zivkovic I, Cvetesic N, Tawfik DS, Toth-Petroczy A, Macek B, Gruic-Sovulj I. 2019. On the Mechanism and Origin of Isoleucyl-tRNA Synthetase Editing against Norvaline. *J Mol Biol* **431**:1284–1297. doi:10.1016/j.jmb.2019.01.029

Bishop AC, Nomanbhoy TK, Schimmel P. 2002. Blocking site-to-site translocation of a misactivated amino acid by mutation of a class I tRNA synthetase. *Proc Natl Acad Sci USA* **99**:585–590. doi:10.1073/pnas.012611299

Calendar R, Berg P. 1966. Purification and Physical Characterization of Tyrosyl Ribonucleic Acid Synthetases form Escherichia coli and Bacillus subtilis. *Biochemistry* **5**:1681–1690. doi:10.1016/B978-0-12-384730-0.00100-2

Cole FX, Schimmel PR. 1970. On the Rate Law and Mechanism of the Adenosine Triphosphate–Pyrophosphate Isotope Exchange Reaction of Amino Acyl Transfer Ribonucleic Acid Synthetases. *Biochemistry* **9**:480–489. doi:10.1021/bi00805a005

Cvetesic N, Akmačić I, Gruic-Sovulj I. 2013. Lack of discrimination against non-proteinogenic amino acid norvaline by elongation factor Tu from Escherichia coli. *Croat Chem Acta* **86**:73–82. doi:10.5562/cca2173

Cvetesic N, Bilus M, Gruic-Sovulj I. 2015. The tRNA A76 hydroxyl groups control partitioning of the tRNA-dependent pre- and post-transfer editing pathways in class I tRNA synthetase. *J Biol Chem* **290**:13981–13991. doi:10.1074/jbc.M115.648568

Cvetesic N, Gruic-Sovulj I. 2017. Synthetic and editing reactions of aminoacyl-tRNA synthetases using cognate and non-cognate amino acid substrates. *Methods* **113**:13–26. doi:10.1016/j.ymeth.2016.09.015

Cvetesic N, Palencia A, Halasz I, Cusack S, Gruic-Sovulj I. 2014. The physiological target for LeuRS translational quality control is norvaline. *EMBO J* **33**:1639–1653. doi:10.15252/embj.201488199

Cvetesic N, Perona JJ, Gruic-Sovulj I. 2012. Kinetic partitioning between synthetic and editing pathways in class I aminoacyl-tRNA synthetases occurs at both pre-transfer and post-transfer hydrolytic steps. *J Biol Chem* **287**:25381–25394. doi:10.1074/jbc.M112.372151

Dulic M, Cvetesic N, Perona JJ, Gruic-Sovulj I. 2010. Partitioning of tRNA-dependent editing between pre- and post-transfer pathways in class I aminoacyl-tRNA synthetases. *J Biol Chem* **285**:23799–23809. doi:10.1074/jbc.M110.133553

Dulic M, Cvetesic N, Zivkovic I, Palencia A, Cusack S, Bertosa B, Gruic-Sovulj I. 2017. Kinetic Origin of Substrate Specificity in Post-Transfer Editing by Leucyl-tRNA Synthetase. *J Mol Biol* **430**:1–16.

doi:10.1016/j.jmb.2017.10.024

Dulic M, Perona JJ, Gruic-Sovulj I. 2014. Determinants for tRNA-dependent pretransfer editing in the synthetic site of isoleucyl-tRNA synthetase. *Biochemistry* **53**:6189–6198. doi:10.1021/bi5007699

Durairaj P, Hur JS, Yun H. 2016. Versatile biocatalysis of fungal cytochrome P450 monooxygenases. *Microb Cell Fact* **15**:1–16. doi:10.1186/s12934-016-0523-6

Dwivedi S, Kruparani SP, Sankaranarayanan R. 2005. A D-amino acid editing module coupled to the translational apparatus in archaea. *Nat Struct Mol Biol* **12**:556–557. doi:10.1038/nsmb943

Eriani G, Delarue M, Poch O, Gangloff J, Moras D. 1990. Partition of tRNA synthetases into two classes based on mutually exclusive sets of sequence motifs. *Nature* **347**:203–206. doi:10.1038/347203a0

Fersht AR. 1977. Editing Mechanisms in Protein Synthesis. Rejection of Valine by the Isoleucyl-tRNA Synthetase. *Biochemistry* **16**:1025–1030. doi:10.1021/bi00624a034

Fersht AR, Dingwall C. 1979a. Evidence for the double-sieve editing mechanism in protein synthesis. Steric exclusion of isoleucine by valyl-tRNA synthetases. *Biochemistry* **18**:2627–2631. doi:10.1021/BI00579A030

Fersht AR, Dingwall C. 1979b. An Editing Mechanism for the Methionyl-tRNA Synthetase in the Selection of Amino Acids in Protein Synthesis. *Biochemistry* **18**:1250–1256. doi:10.1021/bi00574a021

Fersht AR, Kaethner MM. 1976. Enzyme Hyperspecificity. Rejection of Threonine by the Valyl-tRNA Synthetase by Misacylation and Hydrolytic Editing. *Biochemistry* **15**:3342–3346. doi:10.1021/bi00660a026

Fersht AR, Shi J-P, Knill-Jones JW, Lowe DM, Wilkinson AJ, Blow DM, Brick P, Carter P, Waye MMY, Winter G. 1985. Hydrogen bonding and biological specificity analysed by protein engineering. *Nature* **314**:235–238. doi:10.1038/315279a0

Francklyn CS, First EA, Perona JJ, Hou Y-MM. 2008. Methods for kinetic and thermodynamic analysis of aminoacyl-tRNA synthetases. *Methods* **44**:100–118. doi:10.1016/j.ymeth.2007.09.007

Fukunaga R, Yokoyama S. 2006. Structural basis for substrate recognition by the editing domain of isoleucyl-tRNA synthetase. *J Mol Biol* **359**:901–912. doi:10.1016/j.jmb.2006.04.025

Gomez MAR, Ibba M. 2020. Aminoacyl-tRNA Synthetases. *RNA* **26**:910–936.

Gruic-Sovulj I, Rokov-Plavec J, Weygand-Durasevic I. 2007. Hydrolysis of non-cognate aminoacyl-adenylates by a class II aminoacyl-tRNA synthetase lacking an editing domain. *FEBS Lett* **581**:5110–5114. doi:10.1016/j.febslet.2007.09.058

Hendrickson TL, Nomanbhoy TK, De Crécy-Lagard V, Fukai S, Nureki O, Yokoyama S, Schimmel P. 2002. Mutational separation of two pathways for editing by a class I tRNA synthetase. *Mol Cell* **9**:353–362. doi:10.1016/S1097-2765(02)00449-5

Hussain T, Kamarthapu V, Kruparani SP, Deshmukh M V., Sankaranarayanan R. 2010. Mechanistic insights into cognate substrate discrimination during proofreading in translation. *Proc Natl Acad Sci U S A* **107**:22117–22121. doi:10.1073/pnas.1014299107

Jakubowski H, Fersht AR. 1981. Alternative pathways for editing non-cognate amino acids by aminoacyl-tRNA synthetases. *Nucleic Acids Res* **9**:3105–3117. doi:10.1093/nar/9.13.3105

Johnson KA. 2019. New standards for collecting and fitting steady state kinetic data. *Beilstein J Org Chem* **15**:16–29. doi:10.3762/bjoc.15.2

Johnson KA. 2008. Role of induced fit in enzyme specificity: A molecular forward/reverse switch. *J Biol Chem* **283**:26297–26301. doi:10.1074/jbc.R800034200

Kotik-Kogan O, Moor N, Tworowski D, Safro M. 2005. Structural basis for discrimination of L-phenylalanine from L-tyrosine by phenylalanyl-tRNA synthetase. *Structure* **13**:1799–1807. doi:10.1016/j.str.2005.08.013

Kourouklis D, Murakami H, Suga H. 2005. Programmable ribozymes for mischarging tRNA with nonnatural amino acids and their applications to translation. *Methods* **36**:239–244. doi:10.1016/j.ymeth.2005.04.001

LaRiviere FJ, Wolfson AD, Uhlenbeck OC. 2001. Uniform binding of aminoacyl-tRNAs to elongation factor Tu by thermodynamic compensation. *Science* **294**:165–168. doi:10.1126/science.1064242

Lee JW, Beebe K, Nangle LA, Jang J, Longo-Guess CM, Cook SA, Davisson MT, Sundberg JP, Schimmel P, Ackerman SL. 2006. Editing-defective tRNA synthetase causes protein misfolding and neurodegeneration. *Nature* **443**:50–55. doi:10.1038/nature05096

Lin L, Hale SP, Schimmel P. 1996. Aminoacylation Error Correction. *Nature* **384**:33–34. doi:10.1038/384033b0

Ling J, Roy H, Ibba M. 2007a. Mechanism of tRNA-dependent editing in translational quality control. *Proc Natl Acad Sci U S A* **104**:72–77. doi:10.1073/pnas.0606272104

Ling J, So BR, Yadavalli SS, Roy H, Shoji S, Fredrick K, Musier-Forsyth K, Ibba M. 2009. Resampling and Editing of Mischarged tRNA Prior to Translation Elongation. *Mol Cell* **33**:654–660. doi:10.1016/j.molcel.2009.01.031

Ling J, Yadavalli SS, Ibba M. 2007b. Phenylalanyl-tRNA synthetase editing defects result in efficient mistranslation of phenylalanine codons as tyrosine. *Rna* **13**:1881–1886. doi:10.1261/rna.684107

Liu Z, Vargas-Rodriguez O, Goto Y, Novoa EM, Ribas De Pouplana L, Suga H, Musier-Forsyth K. 2015. Homologous trans-editing factors with broad tRNA specificity prevent mistranslation caused by serine/threonine misactivation. *Proc Natl Acad Sci U S A* **112**:6027–6032. doi:10.1073/pnas.1423664112

Loftfield RB, Vanderjagt D. 1972. The frequency of errors in protein biosynthesis. *Biochem J* **128**:1353–1356. doi:10.1042/BJ1281353

Minajigi A, Francklyn CS. 2008. RNA-assisted catalysis in a protein enzyme: The 2'-hydroxyl of tRNAThr A76 promotes aminoacylation by threonyl-tRNA synthetase. *Proc Natl Acad Sci U S A* **105**:17748–17753. doi:10.1073/pnas.0804247105

Nakama T, Nureki O, Yokoyama S. 2001. Structural Basis for the Recognition of Isoleucyl-Adenylate and an Antibiotic, Mupirocin, by Isoleucyl-tRNA Synthetase. *J Biol Chem* **276**:47387–47393. doi:10.1074/jbc.M109089200

Nazarenko IA, Harrington KM, Uhlenbeck OC. 1994. Many of the conserved nucleotides of tRNA(Phe) are not essential for ternary complex formation and peptide elongation. *EMBO J* **13**:2464–2471. doi:10.1002/j.1460-2075.1994.tb06531.x

Newberry KJ, Hou YM, Perona JJ. 2002. Structural origins of amino acid selection without editing by cysteinyl-tRNA synthetase. *EMBO J* **21**:2778–2787. doi:10.1093/emboj/21.11.2778

Nureki O, Niimi T, Muramatsu T, Kanno H, Kohno T, Florentz C, Giege R, Yokoyama S. 1994. Molecular Recognition of the Identity-determinant Set of Isoleucine Transfer RNA from Escherichia coli. *J Mol Biol* **236**:710–724. doi:10.1006/jmbi.1994.1184

Palencia A, Crépin T, Vu MT, Lincecum TL, Martinis SA, Cusack S. 2012. Structural dynamics of the aminoacylation and proofreading functional cycle of bacterial leucyl-tRNA synthetase. *Nat Struct Mol Biol* **19**:677–684. doi:10.1038/nsmb.2317

Perona JJ, Gruic-Sovulj I. 2014. Synthetic and editing mechanisms of aminoacyl-tRNA synthetases. *Top Curr Chem*. doi:10.1007/128_2013_456

Ribas de Pouplana L, Schimmel P. 2001. Two classes of tRNA synthetases suggested by sterically compatible dockings on tRNA acceptor stem. *Cell* **104**:191–193. doi:10.1016/S0092-8674(01)00204-5

Routh SB, Pawar KI, Ahmad S, Singh S, Suma K, Kumar M, Kuncha SK, Yadav K, Kruparani SP, Sankaranarayanan R. 2016. Elongation Factor Tu Prevents Misediting of Gly-tRNA(Gly) Caused by the Design Behind the Chiral Proofreading Site of D-Aminoacyl-tRNA Deacylase. *PLoS Biol* **14**:1–22. doi:10.1371/journal.pbio.1002465

Sanderson LE, Uhlenbeck OC. 2007. Directed Mutagenesis Identifies Amino Acid Residues Involved in Elongation Factor Tu Binding to yeast Phe-tRNAPhe. *J Mol Biol* **368**:119–130. doi:10.1016/j.jmb.2007.01.075

Sankaranarayanan R, Dock-Bregeon AC, Rees B, Bovee M, Caillet J, Romby P, Francklyn CS, Moras D. 2000. Zinc ion mediated amino acid discrimination by threonyl-tRNA synthetase. *Nat Struct Biol* **7**:461–465. doi:10.1038/75856

Silvian LF, Wang J, Steitz TA. 1999. Insights into editing from an Ile-tRNA synthetase structure with tRNA(Ile) and mupirocin. *Science* **285**:1074–1077. doi:10.1126/science.285.5430.1074

Tardif KD, Liu M, Vitseva O, Hou YM, Horowitz J. 2001. Misacylation and editing by Escherichia coli valyl-tRNA synthetase: Evidence for two tRNA binding sites. *Biochemistry* **40**:8118–8125. doi:10.1021/bi0103213

Tawfik DS. 2014. Accuracy-rate tradeoffs: How do enzymes meet demands of selectivity and catalytic efficiency? *Curr Opin Chem Biol* **21**:73–80. doi:10.1016/j.cbpa.2014.05.008

Tawfik DS, Gruic-Sovulj I. 2020. How evolution shapes enzyme selectivity – lessons from aminoacyl-tRNA synthetases and other amino acid utilizing enzymes. *FEBS J* **287**:1284–1305.

Vögeli B, Erb TJ. 2018. 'Negative' and 'positive catalysis': complementary principles that shape the catalytic landscape of enzymes. *Curr Opin Chem Biol* **47**:94–100. doi:10.1016/j.cbpa.2018.09.013

Wolfson AD, Uhlenbeck OC. 2002. Modulation of tRNAAla identity by inorganic pyrophosphatase. *Proc Natl Acad Sci USA* **99**:5965–5970. doi:10.1073/pnas.092152799

Yarus M. 1972. Phenylalanyl-tRNA synthetase and isoleucyl-tRNA Phe : a possible verification mechanism for aminoacyl-tRNA. *Proc Natl Acad Sci U S A* **69**:1915–1919. doi:10.1073/pnas.69.7.1915

Zhang CM, Perona JJ, Ryu K, Francklyn C, Hou Y-MM. 2006. Distinct Kinetic Mechanisms of the Two Classes of Aminoacyl-tRNA Synthetases. *J Mol Biol* **361**:300–311. doi:10.1016/j.jmb.2006.06.015

Zivkovic I, Moschner J, Koksch B, Gruic-Sovulj I. 2020. Mechanism of discrimination of isoleucyl-tRNA synthetase against nonproteinogenic α-aminobutyrate and its fluorinated analogues. *FEBS J*

287:800–813. doi:10.1111/febs.15053